Bioactive Lactose-Modified Chitosan Acts as a Temporary Extracellular Matrix for the Formation of Chondro-Aggregates

Chiara Pizzolitto, Francesca Scognamiglio,* Giovanna Baldini, Roberta Bortul, Gianluca Turco, Ivan Donati, Vanessa Nicolin, and Eleonora Marsich

ABSTRACT: Spheroids based on chondrocytes are gaining interest in the treatment of injured cartilage tissue due to their regenerative potential. In this study, chondrocyte-based aggregates were formed by culturing cells on a polymeric coating of a lactose-modified chitosan (CTL) and their evolution was followed for 14 days of culture. Morphological analyses through scanning electron microscopy indicated that these cell aggregates formed by a process of cell aggregation rather than proliferation, resulting in structures with an irregular morphology that were up to 1 mm in size. Chondrocytes interact very closely with CTL. In the early days of cellular aggregation, CTL is distributed among the cells, while in later stages, it is localized in the inner part of the aggregates, forming an amorphous matrix. The initial outer position of the polymer is replaced over time by an increased matrix deposition whose main component is type II collagen. Transmission electron microscopy pointed out that the chondrocytes internalized the polymer during the first days of culture. The presence of CTL does not affect the ability of cells to migrate from chondro-aggregates when transferred to uncoated wells, mimicking the ability of cells to colonize a cartilage defect. Overall, these results suggest that CTL plays a role as a temporary matrix for chondrocytes aggregation during chondro-aggregates formation. This opens up innovative therapeutic approaches for cartilage regeneration without the need to use a scaffold to deliver cells to the damaged site.

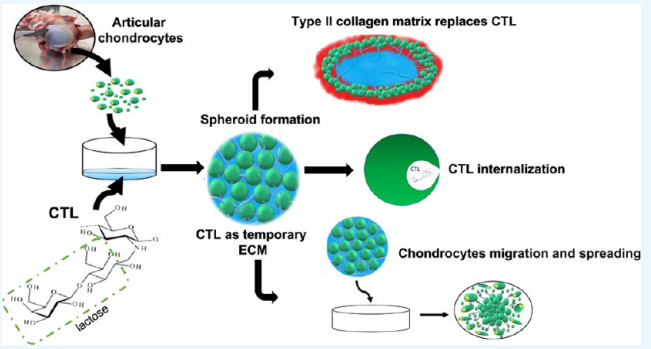

KEYWORDS: *chondrocytes, spheroids, lactose-modified chitosan, cartilage regeneration, bioactive polysaccharide*

1. INTRODUCTION

The regeneration of articular cartilage is still a challenge, and for this reason, articular cartilage diseases are considered one of the most important health problems with an impact on the quality of life.[1,2] Several approaches have been developed over the years, but there are still many limitations that need to be addressed.[3] For example, the successful results of some techniques (microfractures, autologous chondrocyte implantation (ACI), matrix-induced autologous chondrocyte implantation (MACI), or autologous matrix-induced chondrogenesis (AMIC)) can be compromised by some drawbacks, such as a two-step surgery for some of them, the limited size of the defect that can be restored, and the formation of fibrocartilage tissue, rich in type I collagen.[4] Despite several commercial products for cartilage regeneration launched on the market,[5−7] in recent years great expectations have been placed on cell therapy.[8] Interest in scaffold-free culture strategies is steadily growing, and many of them are already used in clinical practice.[4,9] Two main types of cells are used for this therapeutic approach: chondrocytes and mesenchymal stem cells (MSCs). ACI, for example, is a two-stage procedure based on the use of chondrocytes from patients. In the first operation, chondrocytes are taken from a biopsy of healthy cartilage and expanded *in vitro* for a few weeks. The patient then undergoes a second operation in which autologous chondrocytes are implanted into the defect site, which is covered by a periosteum graft. Although many results are satisfactory, the possibility of hypertrophy of the grafted periosteum and dedifferentiation during *in vitro* culture in two-dimensional (2D) can compromise or even derail this procedure.[10−12]

To overcome these problems, chondrocytes must be cultured in a three-dimensional (3D) environment. Culturing chondrocytes in spheroidal forms has already been used successfully. As reported by Vonk and co-authors, the formation of scaffold-free spheroids from patients' chondrocytes is a validated procedure used in Germany for the repair of

articular cartilage defects.[13] To form spheroids, the cells must be cultured in such a way that adhesion of the cells to a surface is prevented.[14−16] In 2005, our research group reported that a lactose-modified chitosan, called Chitlac, in contact with a primary culture of chondrocytes, induces their aggregation with the formation of nodules with large dimensions (up to 0.5−1 mm) and stimulates the production of type II collagen and glycosaminoglycans (GAGs).[17] Chitlac is a biocompatible modified polysaccharide consisting of a chitosan backbone into which lactitol moieties have been chemically inserted.[18,19] In vitro studies show that Chitlac promotes the expression of cartilage matrix components in primary chondrocytes within an otherwise inert 3D architecture,[20] displays good reactive oxygen species (ROS) scavenger activity,[21] and that, in combination with hyaluronic acid (HA), it attenuates inflammation, inhibits the expression of matrix metalloproteinases (MMPs), and has antioxidant effects in inflamed primary human chondrocytes.[22]

Recently, *in vivo* studies have shown that intra-articular injections of Chitlac associated with HA exert chondroprotective and proregenerative effects in rat knee osteoarthritis model.[23,24]

Chitlac, hereinafter referred to as CTL, has been reported to bind the membrane protein galectin-1 (Gal-1), presumably due to the pending lactitol residues.[25,26] There is increasing evidence that correlates the expression of Gal-1 with the degree of cartilage degeneration, with this protein being specifically present at sites of damage.[27] Recent work has shown that the treatment of osteoarthritic chondrocytes with lactose inhibits the binding of Gal-1 to the cell surface. In this way, the expression of Gal-1-regulated genes is reduced, leading to a decrease in inflammation.[28] Since CTL has been demonstrated to be able to inhibit the expression of galectin proteins both *in vivo* and *in vitro*,[23,24,29,30] there is a growing interest in the use of this polymer for the production of materials to be used in the field of cartilage regeneration.[21,31]

In this study, chondro-aggregates are assembled in the presence of the polysaccharide CTL to form hybrid cell/polymer structures. The aggregates are characterized from a structural and biological point of view and show a close molecular interaction between the cellular component and the polysaccharide. CTL is localized within the nodule as a temporary biological matrix that controls the formation and the morphological development of the aggregates. The external and internal morphologies of the chondro-aggregates, polymer localization, extracellular matrix (ECM) synthesis, and the ability of cells to migrate out of the aggregates are investigated over time. Overall, these results address the CTL-based chondro-aggregates as an innovative form of cell therapy system for defective cartilage that combines the implantation of chondrocytes with *in situ* delivery of a proregenerative bioactive polymer.

2. MATERIALS AND METHODS

2.1. Materials. The hydrochloride form of lactose-modified chitosan, CTL (CAS Registry Number 2173421.37-7), with fractions of *N*-acetyl-glucosamine (GlcNAc; "acetylated", A) (F_A) = 0.16; glucosamine ($GlcNH_2$; "deacetylated", D) (F_D) = 0.21; and lactitol-substituted D unit (*N*-alkylated GlcLac; "lactitol", L) (F_L) = 0.63, was kindly provided by Biopolife S.r.L. (Trieste, Italy). The intrinsic viscosity [η] determined at 25 °C by viscosimetry (CT1150 Schott Geräte automatic measuring apparatus and a Schott capillary viscometer) was 344 mL/g, and the estimated molecular weight was 780000 g/mol.[31] Phosphate-buffered saline (PBS), Triton X-100, type I-S hyaluronidase from bovine testes, collagenase type II, Toluidine Blue, Alcian Blue, sodium hydroxide (NaOH), formaldehyde, bovine serum albumin (BSA), poly(vinyl alcohol) (MOWIOL 4-88), normal goat serum (NGS), and TRI reagent, FITC, were all purchased from Sigma-Aldrich. Dulbecco's modified Eagle's medium (DMEM), penicillin/streptomycin, trypsin-ethylenediaminetetraacetic acid (EDTA) 1×, and fetal bovine serum (FBS) were purchased from EuroClone s.p.a. Acetic acid glacial and ethanol were purchased from Carlo Erba. L-Ascorbic acid was from Fluka Biochemika. Transforming growth factor β 1 (TGFβ1) was purchased from Abcam. Collagen II monoclonal antibody (2B1.5) (catalog number #MA5-12789), collagen I monoclonal antibody (COL-1) (catalog number #MA1-26771), goat antimouse IgG (H+L) highly cross-adsorbed secondary antibody, and Alexa Fluor 594 (catalog number #A-11032) were all from Thermo Fisher Scientific. Hoechst was from Invitrogen (Bleiswijk, The Netherlands). Killik, O.C.T. compound embedding medium for cryostat, and Sirius Red Picrate were from Bio-Optica (Milan, Italy).

2.2. Isolation and Expansion of Pig Articular Chondrocytes. Primary chondrocytes were isolated according to a procedure previously described by Grandolfo et al.[32] from intact joints of adult pigs provided by a local slaughterhouse. After dislocation of the joints, the cartilage was washed with 1× sterile PBS. Thin slices of the cartilage were cut with a sterile scalpel, and the cells were isolated by the enzymatic digestion of the tissue. The cartilage slices were digested for 1 h in 15 mL of hyaluronidase solution (hyaluronidases 250 U/mL, penicillin 500 U/mL, and streptomycin 500 U/mL in 1× PBS) at 37 °C, 5% CO_2 in a humidified environment. Tissue digestion was completed by overnight incubation with 10 mL of collagenase solution (collagenase type II 250 U/mL, penicillin 500 U/mL, and streptomycin 500 U/mL in 1× PBS) at 37 °C under vigorous shaking. Enzymes and digestion products were removed by running the mixture through a sieve. Finally, the cells were washed with 1× PBS and with DMEM. Chondrocytes were seeded in flasks and cultured in DMEM high glucose supplemented with 10% FBS and 1% penicillin/streptomycin. The cells were incubated at 37 °C in a humidified environment with 5% CO_2 for 1 day to avoid cell dedifferentiation and then used for chondro-aggregates formation.

2.3. Chondro-Aggregates Formation. To induce the formation of aggregates, the protocol described by Donati et al. was used.[17] Briefly, 400 μL of a 2% w/v CTL solution in 1× PBS, pH 7.4 was homogeneously distributed over the bottom of a well of a 24-well plate and allowed to air-dry overnight. The coated wells were sterilized by UV irradiation for 30 min. Primary chondrocytes were seeded at a final density of 6×10^4 cells/well and maintained in culture for a maximum period of 14 days. The medium was changed every 4 days. The cell medium (DMEM high glucose supplemented with 10% FBS and 1% penicillin/streptomycin) was enriched with ascorbic acid (50 μg/mL) and TGFβ1 (0.05 ng/mL).

2.4. Cytotoxicity and Viability Analysis (MTT/LDH/Live Dead). Cell viability was determined using the 3,4,5-dimethylthiazol-2yl-2,5-diphenyltetrazolium bromide (MTT) assay. At selected time points, the entire content of each well was transferred to a vial, washed with 1× PBS, and incubated with 300 μL of MTT solution (0.5 mg/mL) for 4 h at 37 °C in the dark. After incubation, the MTT solution was removed and 100 μL of dimethyl sulfoxide (DMSO) was added to each vial to dissolve the formazan crystals. The absorbance of each sample was measured at 570 nm using a FLUOStar Omega-BMG Labtech spectrophotometer.

To assess the suffering of the cells, the release of lactose dehydrogenase (LDH) into the culture medium was measured using the "*In Vitro* Toxicology Assay Kit, Lactic Dehydrogenase bases" (SIGMA) according to the manufacturer's instructions.

The viability of the aggregates was also analyzed qualitatively using a Live/Dead Assay Kit (SIGMA). For this analysis, 2 μL of solution A (containing calcein-AM) and 1 μL of solution B (containing propidium iodide) were added to 1 mL of 1× PBS. Then, 100 μL of the resulting mixture was added to the sample. Images were captured using a Nikon Eclipse Ti-E epifluorescence live-imaging microscope equipped with a motorized stand and a Nikon DS-Qi2

camera. Images were taken using Nis-Elements 4.60 software and 10× objective after the incubation of samples for 15 min in the dark at 37 °C in a humidified environment.

2.5. External Morphological Analysis. External morphological analyses of the chondro-aggregates were performed by scanning electron microscopy (SEM, Quanta 250, FEI, Oregon). At selected time points, aggregates were washed with 1× PBS and fixed with 2.5% (w/v) glutaraldehyde in 1× PBS at room temperature for 1 h. The fixative was removed by washing the aggregates with 1× PBS. The aggregates were gradually dehydrated in ethanol (30−70−100%) and finally dried using a critical point dryer (HMDS). Each step was performed twice (20 min each), and between each step, the samples were centrifugated at 69*g* for 5 min to collect nodules. Prior to SEM analysis, the dehydrated samples were gold-sputtered (Sputter Coater K550X, Emitech, Quorum Technologies Ltd., U.K.).

2.6. Transmission Electron Microscopy (TEM) and Toluidine Blue Staining. Pellets of chondro-aggregates were fixed in 2.5% glutaraldehyde EM grade in 0.1 M phosphate buffer, pH 7.3 and postfixed in 1% osmium tetroxide. Samples were dehydrated through a graded series of ethanol and finally in propylene oxide and then embedded in epoxy resin (Durcupan ACM, Sigma-Aldrich). Ultrathin sections (60−80 nm) were placed on copper grids, stained with UranyLess EM stain (a substitute for uranyl acetate) and lead citrate, and observed with a transmission electron microscope (Philips EM 208 at 100 kV); images were acquired with a Quemesa bottom-mounted TEM CCD camera (Olympus, Germany) provided with a TEM imaging platform (Radius software). All of the reagents were from Electron Microscopy Sciences, Hatfield, PA. The resin-embedded samples were also cut with an ultramicrotome to obtain semifine sections of 1 μm and then hot-stained with Toluidine Blue.

2.7. Preparation of Sample for Internal Characterization. For internal histological analyses, chondro-aggregates were pre-embedded in 1.5% w/v agarose in 1× PBS. Gels were then fixed with 4% formaldehyde for 30 min, washed with 1× PBS, and incubated overnight in 30% sucrose at 4 °C. Then, gels were incubated in a mixture containing 50% sucrose (concentration = 30%) and 50% OCT for 5 h. Finally, gels were embedded in OCT and incubated at −20 °C to allow sample freezing.[33] The frozen gels were sectioned by a cryotome (LEICA CM3050 S.) to obtain slices of a thickness of 50 μm and stained following standard histological and immunohistochemical protocols.

2.8. Analysis of CTL Distribution. Chondro-aggregates were prepared with 10% w/W fluorescein isothiocyanate (FITC)-labeled CTL to analyze polymer distribution both outside and inside the structure. Fluorescein isothiocyanate (FITC)-labeled CTL was prepared following the protocol described by Sacco et al.[34] Briefly, CTL (500 mg) was dissolved in 167 mL of deionized water under stirring conditions overnight and 1.1 mL of FITC solution (0.5 mg/mL in sodium bicarbonate buffer, 50 mM) was added under stirring. The reaction mixture was protected from light and stirred for 24 h at room temperature. After that, the CTL−FITC solution was dialyzed (Spectrapore, MWCO 12′000) against 50 mM $NaHCO_3$, 100 mM NaCl, and later against deionized water until the conductance was below 3 μS/cm at 4 °C. Finally, the pH of the solution was adjusted to 4.5 and freeze-dried using an ALPHA 1−2 LD plus freeze-dryer (CHRIST, Osterode am Harz, Germany).

For external analysis, the chondro-aggregates were collected and fixed with 4% v/v formaldehyde in 1× PBS for 10 min at room temperature. Then, the samples were washed 3 times with 1× PBS and permeabilized with 0.2% v/v Triton in 1× PBS for 15 min at room temperature. Subsequently, they were washed with 1× PBS and incubated with 4% w/v BSA and 5% v/v NGS in 1× PBS (blocking solution) for 1 h at 37 °C. The blocking solution was then removed, and the samples were washed with 1× PBS. For visualization of nuclei, cells were counterstained with 1:1000 Hoechst in PBS. Images were acquired with a Nikon Eclipse Ti-E epifluorescence live-imaging microscope using 10× as objective.

The same protocol was used for the internal characterization of the chondro-aggregates. In this case, aggregates were prepared according to the protocol described in Section 2.7.

2.9. Preparation of Different Culture Conditions for the Assessment of Internalization of CTL by Chondrocytes. To assess the internalization of CTL into cells, chondrocytes were cultured in three different conditions. In the first method, chondrocytes were seeded in a 2D system at a density of 6×10^4 cells/well on a 24-well plate. In the second case, nonadhesive agar-coated wells were used to induce spheroid formation in the absence of CTL.[35,36] For the agar coating, 400 μL of a solution of 2% w/v agar in 1× PBS was poured into a 24-well plate. After 30 min, 6×10^4 cells/well were seeded atop the coating. In these two cases, cells were treated with DMEM supplemented with 10% FBS, 1% penicillin/streptomycin, ascorbic acid (50 μg/mL), and TGFβ1 (0.05 ng/mL). In the last case, 2D-chondrocytes were cultured in DMEM supplemented with not only 10% FBS, 1% penicillin/streptomycin, ascorbic acid (50 μg/mL), and TGFβ1 (0.05 ng/mL) but also 0.5% w/v CTL. For all of the conditions, chondrocytes were cultured for 3 days, collected, and processed for TEM analyses, as described in Section 2.6.

2.10. FACS Analysis and Confocal Laser Microscopy for Determination of CTL Internalization. Chondrocytes were seeded in 6-well plates at a density of 1×10^6 cells per well and incubated for 24 h with 1% (w/v) CTL labeled with FITC in complete medium (DMEM supplemented with 10% FBS and 1% penicillin/streptomycin). Untreated cells were used as control. Chondrocytes were then washed twice with 1× PBS, scraped, centrifuged, and resuspended in 500 μL of 1× PBS. An initial cytofluorimeter analysis was performed with the unmodified cell suspension. Then, trypan blue (final concentration = 0.1% w/v) was added to the suspension and another measurement was performed after 2 min.

Flow cytometric analyses were performed using the Cytomics FC500 instrument (Beckman-Coulter Inc., Fullerton, CA) equipped with an argon laser (488 nm, 5 mV) and a standard configuration system for detection with filters in the channel red (575 nm, FL2; 610 nm, FL1) and green (525 nm, FL1). At least 10,000 events were recorded for each sample. The FL1 histograms were analyzed using WinMDI software (Dr J. Trotter, Scripps Research Institute, La Jolla, CA) to determine the fluorescence intensity values for each sample, expressed as mean fluorescence intensity (MFI).

For confocal laser microscopy, the cells were treated with CTL−FITC as described above. After 24 h, the chondrocytes were washed with 1× PBS, fixed in 4% (w/v) paraformaldehyde in 1× PBS and cover-slipped with a mounting medium (Mowiol). The samples were analyzed by a confocal laser microscopy (Leica TCS SP2 model) at different Z-stacks.

2.11. Chondro-Aggregates Adhesion and Chondrocyte Migration and Spreading. To analyze the ability of chondro-aggregates to adhere to a surface and subsequently to evaluate the ability of chondrocytes to migrate from the structure and to spread, aggregates were formed and cultured for different periods of time. At different time points, the aggregates were moved in a well of a 24-well plate without changing the culture media. After 7 days, the medium was changed, and the aggregates were cultured for up to 10 days. The process of adhesion of the same aggregates was followed over time using a Nikon Eclipse Ti-E epifluorescence live-imaging microscope.

2.12. Histochemical and Immunohistochemical Analysis of Matrix Depositions. The chondro-aggregate sections for histochemical and immunohistochemical analysis were prepared according to the protocol explained in Section 2.7. Glycosaminoglycans production was assessed by Alcian Blue staining. Sections were washed with deionized water and stained with 3% acetic acid for 5 min and for 1 h with Alcian Blue (pH 2.5). The presence of collagen fibers was assessed using the Sirius Red Picrate kit following the manufacturer's instructions (Bio-Optica). Images were taken using a Zeiss Axiophot microscope (Carl Zeiss, Germany). The presence of collagen was also determined using a standard immunohistochemistry procedure. Sections were washed with 1× PBS, permeabilized with 0.2% v/v Triton X-100 for 10 min at room temperature, and then blocked with blocking buffer containing 4% w/v BSA and 5% v/v NGS in 1× PBS for 2 h at room temperature. The solution was then removed, and the samples were washed with 1× PBS. The following

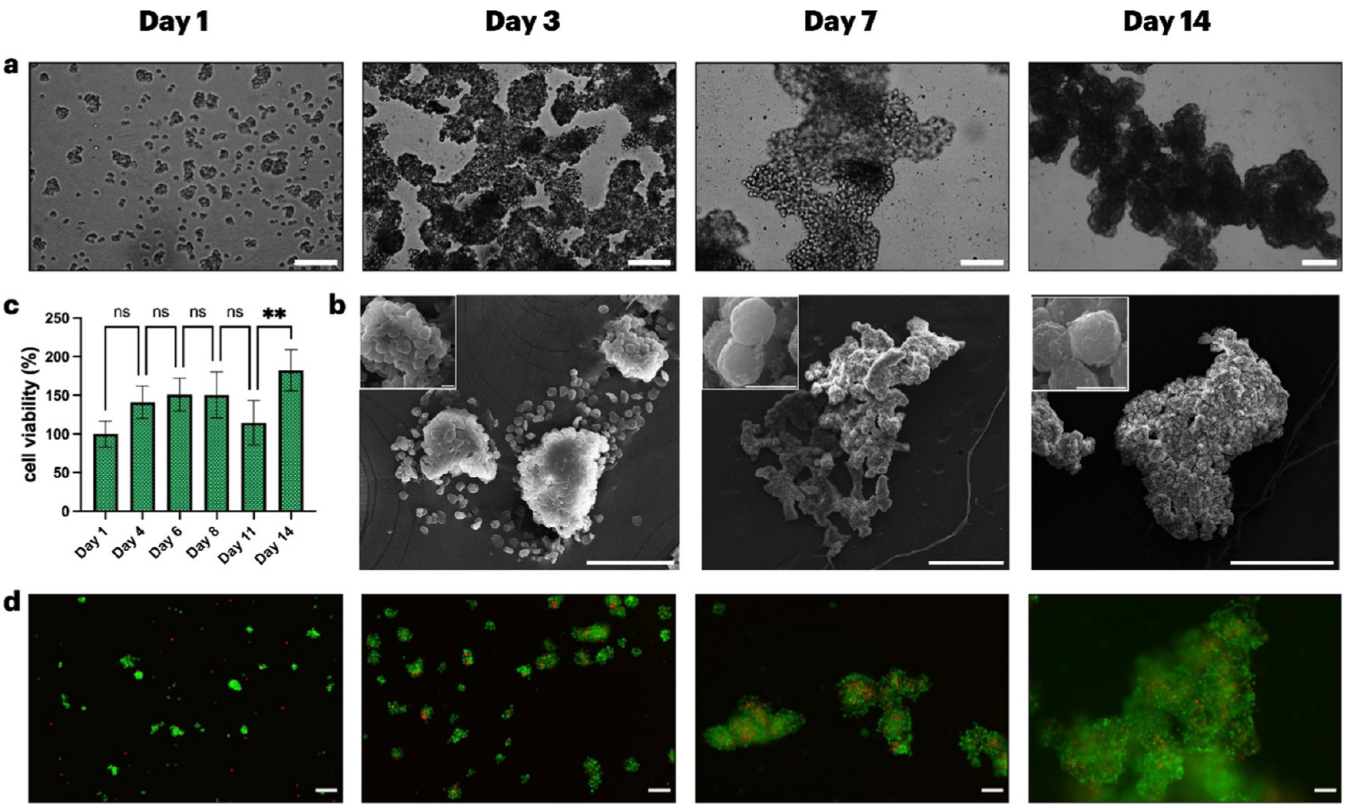

Figure 1. Process of chondro-aggregates formation. (a) Bright-field images of representative chondro-aggregates at different time points. From day 1 to day 7: scale bar 50 μm. Day 14: scale bar 100 μm. (b) SEM images of the chondro-aggregates. Day 3: scale bar 100 μm. Days 7 and 14: scale bars 500 μm. The inset highlights that chondrocytes are embedded in a filamentous matrix that increases over time. For the inset, the scale bar is 10 μm. (c) MTT assay. The percentage of cell viability at day 1 was set at 100%, and the relative viability was calculated for the other selected time points. Results (N = 4) are given as mean ± standard error. Statistics: one-way analysis of variance (ANOVA) followed by Tukey's multiple comparison *post hoc* test; ns, not significant, ** $p < 0.01$. (d) Live/dead cell imaging of chondro-aggregates at different time points. Chondrocytes were stained with two different fluorescent probes to demonstrate cell viability. Dead cells appear red, and living cells appear green.

primary antibodies were used for immunostaining: collagen II monoclonal antibody (1:100), collagen I monoclonal antibody (1:1000). The primary antibodies were diluted in blocking buffer and incubated overnight at 4 °C. Samples were then washed with 1× PBS and incubated with the secondary antibody, Alexa Fluor 594 (1:500). The chondrocyte nuclei were counterstained with Hoechst (1:1000). Images were taken using a Nikon Eclipse Ti-E epifluorescence live-imaging microscope.

2.13. RNA Extraction from Chondro-Aggregates. Chondrocytes were cultured on CTL coating as described in Section 2.3 to allow the formation of chondro-aggregates and collected on days 3 and 7 for RNA extraction. As a reference, RNA extracted from chondrocytes before culturing on CTL coating (day 0) was employed. RNA was extracted from both chondrocyte and chondro-aggregates by using TRI Reagent (Sigma-Aldrich), according to the manufacturer's instructions with some modifications. Chondrocytes and aggregates were incubated with TRI Reagent (1 mL) and centrifugated at 12.000*g* for 10 min at 4 °C. The supernatant was then transferred in a fresh tube and incubated with 0.2 mL of chloroform for 15 min at room temperature. Samples were then centrifugated at 12.000*g* per 20 min at 4 °C to enable phase separation. The aqueous phase containing the RNA was transferred in a fresh tube, and 0.5 mL of 2-propanol was added to the samples. After incubation o/n at −20 °C, the RNA pellet was retrieved by centrifugating at 12.000*g* per 20 min at 4 °C. The supernatant was removed, and the pellet was washed twice in 75% (v/v) ethanol. The RNA pellet was dried for 5 min and resuspended in diethylpyrocarbonate (DEPC) water. The RNA concentration was established by a spectrophotometric analysis at 260−280 nm.

2.14. Reverse Transcription Polymerase Chain Reaction (RT-PCR). RNA extracted from chondrocytes and chondro-aggregates was employed for the synthesis of cDNA by RT-PCR by employing the New England BioLabs reagents. For the reaction, RNA (50 ng) was incubated with a mix containing dNTPs (final concentration = 1 mM) and random primers (final concentration = 10 μM) in a final volume of 10 μL. The samples were incubated at 70 °C per 10 min to prevent the formation of RNA secondary structures. Samples were allowed to stand for 5 min at room temperature. A mix containing M-MLV reverse transcriptase buffer (final concentration = 2×), M-MLV reverse transcriptase enzyme (final concentration = 20 U/μL), and RNase inhibitors (final concentration = 4U/μL) in DEPC water was prepared (final volume = 10 μL). This mix (10 μL) was added to each sample containing the RNA (final volume = 20 μL). RT-PCR was performed at 37 °C for 50 min, followed by an incubation at 85 °C for 10 min for the enzyme inactivation. Samples were stored at −20 °C.

Polymerase chain reaction (PCR) was performed for a qualitative evaluation of collagen1Alpha2 (COL1A2) and collagen2Alpha1 (COL2A1) gene expression on chondrocytes and chondro-aggregates. As a reference, the expression of the housekeeping gene glyceraldehyde-phospho-dehydrogenase (GAPDH) was considered. For the reaction, a mix containing dNTPs (final concentration = 200 μM each), primers forward and reverse (0.2 μM each), Taq polymerase buffer (final concentration = 1X), TAQ polymerase (final concentration = 1.25 U/μL), and cDNA samples (2 μL) in DEPC water (final volume = 50 μL) was prepared. A sample containing all of the reagents without cDNA was employed as a negative control of the reaction. The following amplification steps were considered for cDNA amplification: predenaturation: 95 °C for 30 s, denaturation: 95 °C for 30 s, annealing: 55 °C for 30 s (GAPDH) 57 °C for 30 s (COL2A1), 54 °C for 30 s (COL1A2), extension: 68 °C for 45 s, final extension: 68 °C for 5 min. Amplification was performed for 40 cycles. The primer sequence is

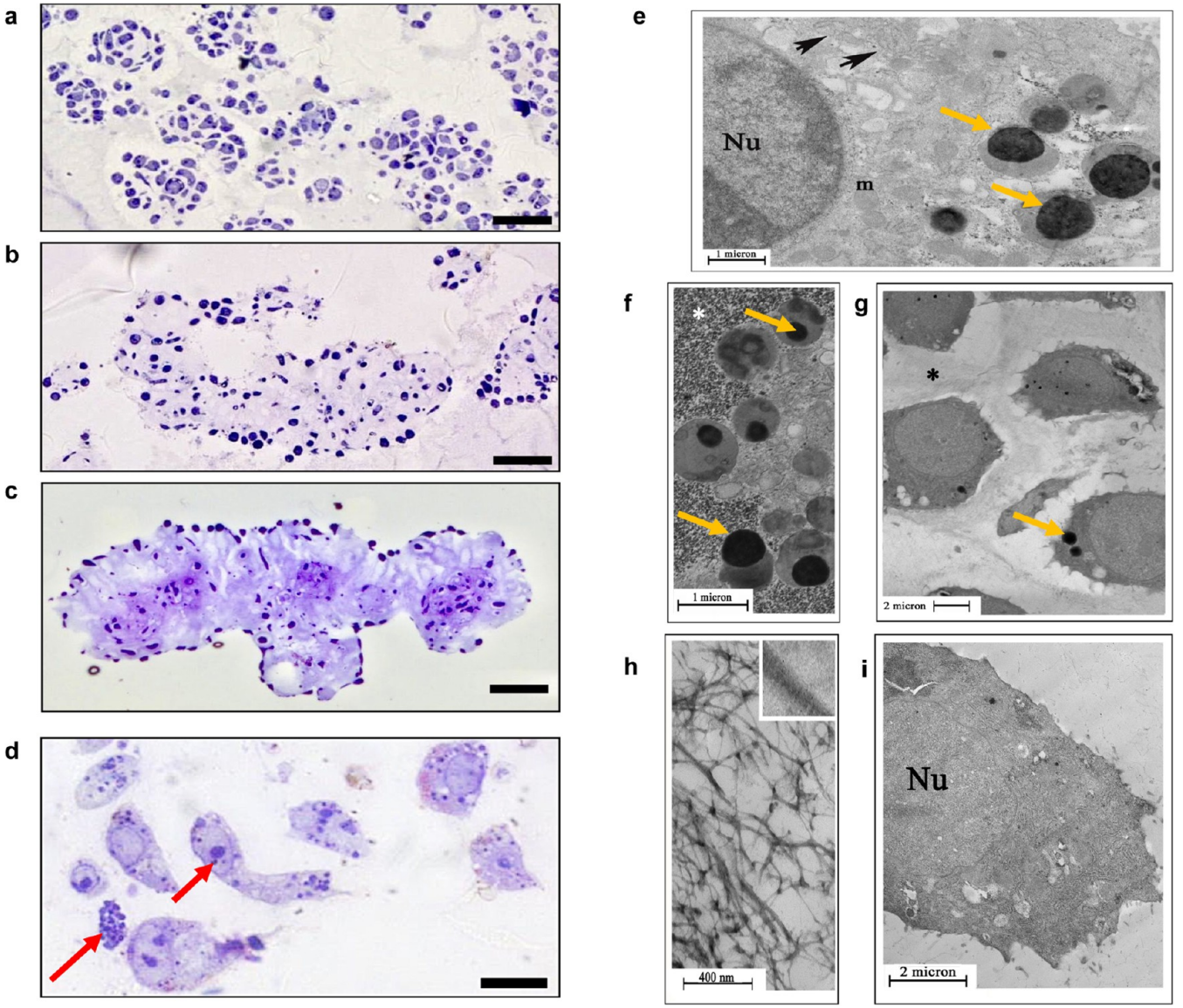

Figure 2. Internal characterization and ultrastructural analysis of chondro-aggregates. (a–d) Optical images of the internal structure of chondro-aggregates stained with Toluidine Blue after 3 days (a), 7 days (b), and 14 days (c) of culture. Scale bar 100 μm. (d) Representative images of Toluidine Blue-positive granular structures (red arrows). Scale bar 10 μm. (e–i) Transmission electron microscopic images at different time points. (e) Chondro-aggregates after 3 days of culture and (f) magnification of their cytoplasmic electrodense vesicles. (g) Chondro-aggregates after 7 days of culture and (h) magnification of their extracellular matrix fibers. (i) Chondro-aggregates after 14 days of culture. Nu, nucleus; m, mitochondria; black arrows, rough endoplasmic reticulum; white asterisk, glycogen granules; black asterisk, extracellular matrix; yellow arrows, electrodense vesicles containing the inclusion material that has a high affinity for osmium.

reported in the Supporting Information (Table S1, Supporting Information). PCR fragments were visualized by electrophoretic analyses on agarose gels (2%) in 1× tris-borate buffer. DNA molecular marker (100 bp DNA ladder NEW ENGLAND BioLabs Inc.; 5 μL) was employed for the evaluation of PCR product dimension. The analysis of the intensity of the PCR fragments for COL2A1, COL1A2, and GAPDH was performed with ImageJ software, and the expression of COL2A1 and COL1A2 was normalized over the expression of GAPDH for each time point.

2.15. Statistical Analysis. Statistical analysis and graph elaboration were performed using GraphPad Prism 9 (GraphPad Software, San Diego, CA). One-way analysis of variance (ANOVA) followed by Tukey's multiple comparison *post hoc* test were performed to evaluate the differences among groups. Differences are considered significant for p-value < 0.05.

3. RESULTS

3.1. External Analysis and Viability of Chondro-Aggregates. To assess the morphology of the chondro-aggregates over time, optical microscopy and SEM images of the structures were taken from day 1 to day 14 after the cells were seeded onto the CTL layer. As can be seen in Figure 1a, numerous loose cell aggregates can be observed as early as 24 h after seeding. They appear to consist of a few cells with the edges within the aggregates still clearly defined. The average diameter of the aggregates is 100 μm. Over time in culture, a progressive increase in the size of the aggregates is observed, reaching an average size of about 1 mm at day 14. The increase in dimensions is accompanied by a progressive decrease in the number of aggregates in the well, a phenomenon clearly due to a process of aggregation of the already formed aggregates, as

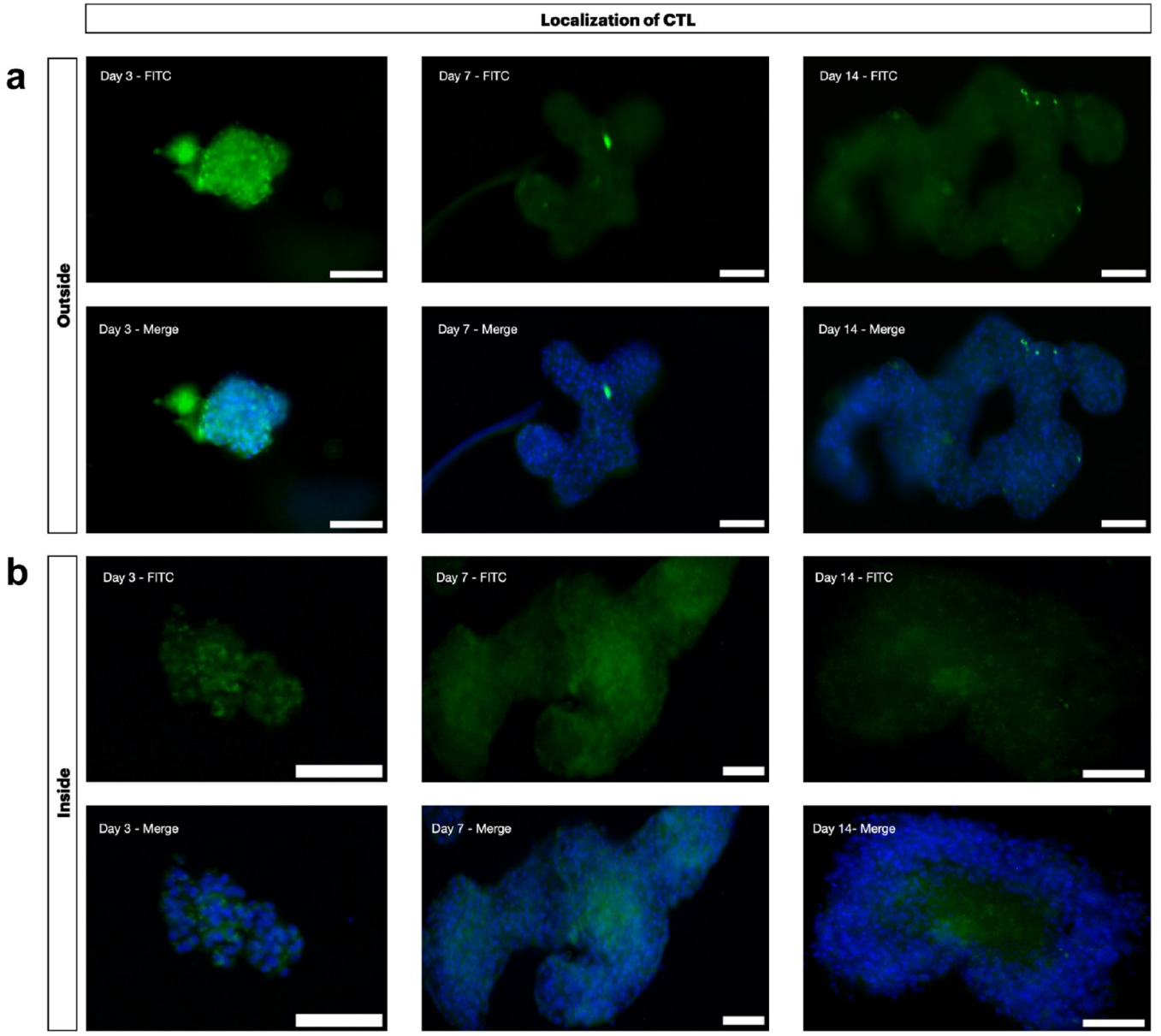

Figure 3. Localization of CTL in chondro-aggregates. Surface localization of CTL (a) and internal localization of CTL (b) at different time points. FITC-labeled CTL was used for polymer localization (green fluorescence); nuclei are stained with Hoechst (blue fluorescence). Scale bars 50 μm.

described in the literature.[14] Moreover, a homogeneous and regular morphology with clearly defined cell boundaries is no longer visible from day 3, and a dark core region can be observed in the larger chondro-aggregates. A crown of cells is only visible at the edge of the aggregates (Figure 1a). The best illustration of the surface morphology of the chondro-aggregates is provided by SEM images (Figure 1b). On day 3, the chondro-aggregates still appear as simple aggregates of single cells. From day 3 to day 14, the shape becomes much more irregular and the individual cells, which are no longer identifiable, appear nested in a granular/fibrous compact structure, most likely due to the presence of a newly synthesized extracellular matrix (inset, Figure 1b).

Chondrocyte viability and proliferation were examined using the MTT assay (Figure 1c). As previously reported by Marcon et al.,[25] the chondrocytes in the spheroids show no replication capacity if we exclude a very low and nonsignificant replication rate between days 1 and 4 of culture. Although there is no significant cell mortality over 14 days, a very slight decrease in cell proliferation is observed at day 11, followed by a weak increase in proliferation at day 14. Furthermore, the extremely low replication of cells in these structures suggests that the increase in the size of the chondro-spheres over time is mainly due to a process of aggregation of preexisting structures.

Further confirmation of these results arises from the live/dead assay. This cytotoxicity test is based on the differential permeability of live and dead cells to a pair of fluorescent stains (calcein-AM stains live cells and propidium iodide for dead cells). As can be seen in Figure 1d, most of the cells on the surface of the chondro-aggregates are viable at all times (green fluorescence cells). From day 3, some dead cells (red fluorescence cells) are observed only in the core of the aggregates. This cellular suffering could be related to the poor diffusion of respiratory gases and nutrients within the aggregates. In addition, the release of lactate dehydrogenase, an enzyme released by cells whose membranes are damaged by

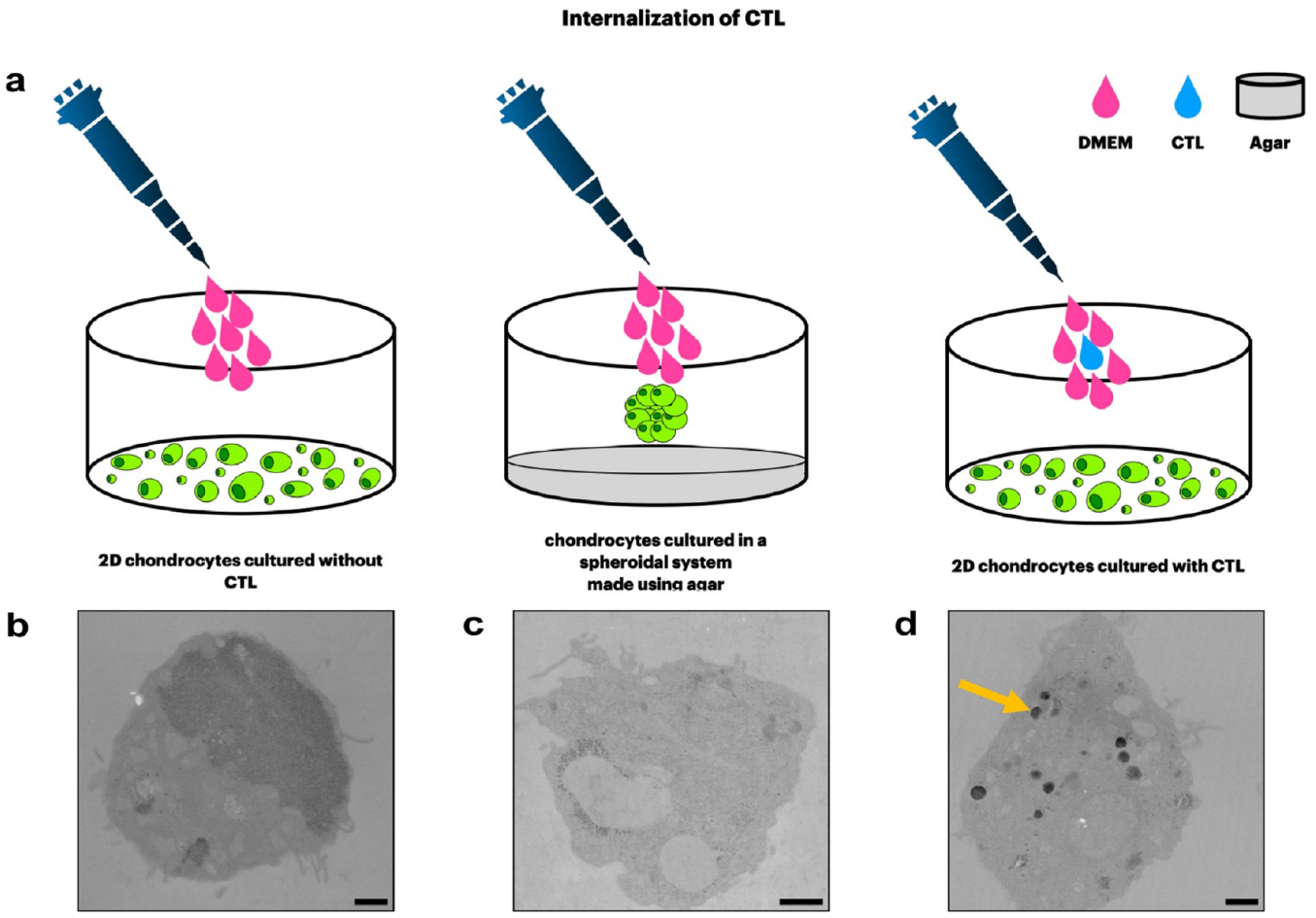

Figure 4. Internalization of CTL. (a) Schematic representation of the sample preparation for microscopy analysis. Chondrocytes were cultured both in the presence and in the absence of CTL. (b–d) TEM images after 3 days of culture of (b) chondrocytes cultured in adhesion in the absence of CTL, (c) spheroids cultured on agar coating in the absence of CTL, and (d) chondrocytes cultured in adhesion in the presence of 0.5% w/v of CTL dissolved in culture medium (scale bars 1 μm. Yellow arrow, electrodense vesicles).

necrosis or apoptosis, is constant in the medium during the 14 days of culture (Figure S1, Supporting Information).

3.2. Internal Characterization and Ultrastructure Analysis of Chondro-Aggregates. The inner structure of the chondro-aggregates was examined after their dissection and staining using standard histological protocols.

Toluidine Blue was used to analyze the distribution of chondrocytes inside the structure. This staining shows a uniform distribution of cells in the aggregates of 3 days (Figure 2a) while, as time progresses and size of the aggregates increases, a gradual process of nodule cavitation is observed. Surprisingly, at day 14, the aggregates consist mainly of a crown of cells bordering a central area poor in cells but rich in an amorphous matrix formed by the polymer CTL, weakly positive for the dye (Figure 2b,c). It is interesting to observe that already from day 3 and onwards the chondrocytes in the nodules are no longer organized in compact cellular structures where the cells are well connected by the formation of tight cell–cell interactions, as can be observed in chondro-aggregates formed in the absence of CTL (Figure S2, Supporting Information) and as reported in the literature.[37] Conversely, large extracellular spaces separate one cell from another. Furthermore, Toluidine Blue staining reveals the presence of small but multiple dye-positive granular structures (red arrows) in the cytoplasm of cells after 3 and 7 days of culture (Figure 2d).

Additional information was obtained using transmission electron microscopy (TEM). Three days after chondro-aggregates formation, the intracellular morphology appears intact, with a well-defined nucleus, numerous mitochondria, and an abundant rough endoplasmic reticulum (black arrows) clearly visible in the cytoplasm (Figure 2e). However, the most striking information provided by ultrastructural analysis is related to the presence of several electrodense vesicles (yellow arrows) containing some intensely osmiophilic materials and surrounded by many glycogen granules (white asterisks), both on days 3 and 7 of culture (Figure 2e,f). These structures may represent the structural analogue of the cytoplasmic granules highlighted by Toluidine Blue in optical microscopy (Figure 2d). On day 7, the filamentous extracellular matrix, which can be identified as newly synthesized mature collagen fibers due to the typical banding (black asterisk), is clearly visible (Figure 2g,h). By day 14, a certain amount of suffering can be observed in the cells, indicated by the vacuolation of the endoplasmic reticulum. In addition, the electrodense vesicles observed in the previous days are no longer visible (Figure 2i). A more detailed discussion of the origin of these electrodense vesicles will be given in the next section.

3.3. Localization of CTL in the Chondro-Aggregates. Evidence of the interaction between CTL and chondrocytes and of the localization of the polymer on the cellular membrane has already been reported by Donati et al.[17]

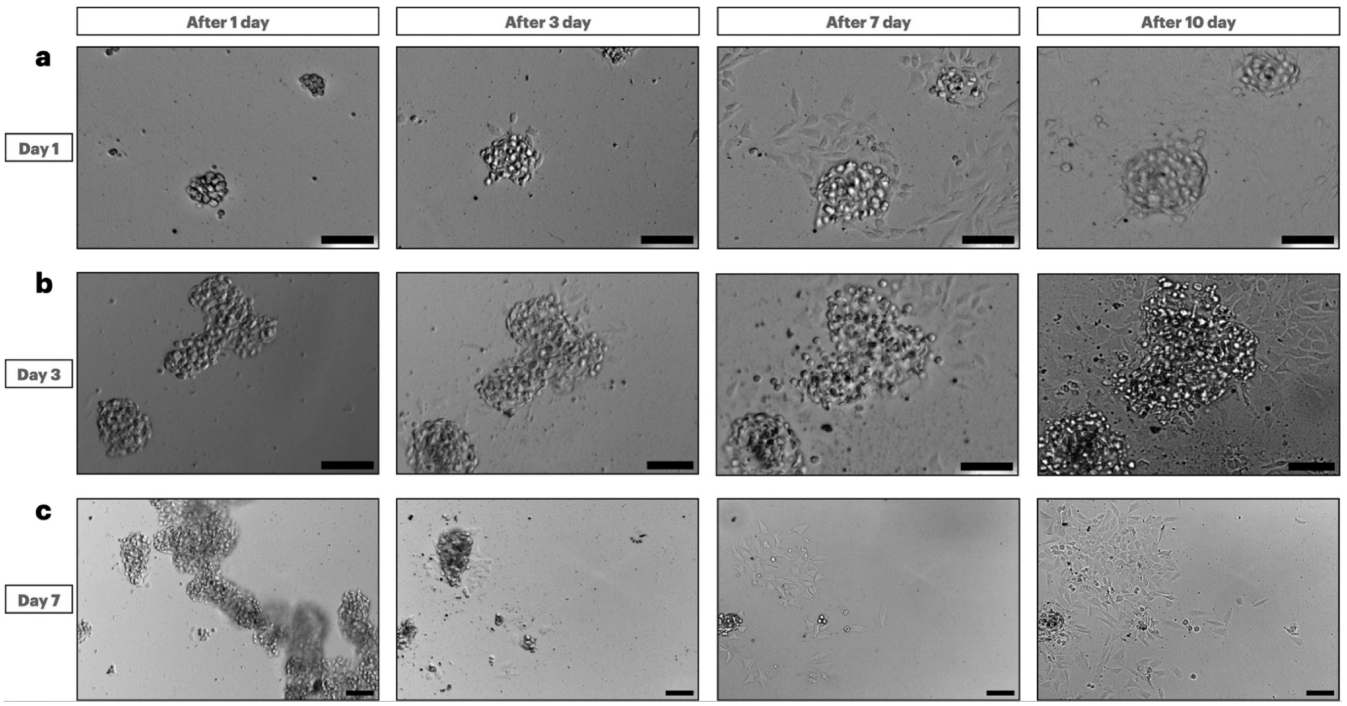

Figure 5. Spreading assay on the adherent surface. Representative bright-field images of chondro-aggregates seeded on adherent substrates followed by cell spreading over 10 days of culture. Chondro-aggregates were transferred 1 (a), 3 (b), and 7 (c) days after assembly on well plates coated with CTL (scale bars 100 μm).

Using CTL labeled with FITC to form aggregates, the present work not only confirms the presence of the polysaccharide on the surface of the nodular structures but also highlights its localization throughout the entire volume of the aggregate in close association with the cellular components (Figure 3a,b). The polysaccharide is visible in the chondro-aggregates until day 14 of cell culture, although a progressive change in its localization can be observed. After 3 days, the polymer is evenly arranged between the cells. From day 7 onwards, in conjunction with the cavitation of the aggregate, the polymer is mainly concentrated in the core of the structure. At the surface of the aggregate and between the individual cells, the fluorescent polymer is no longer visible (Figure 3a,b).

In a previous publication, Marcon et al.[25] reported that Gal-1 acts as a molecular bridge between the chondrocyte and the CTL, mediating the tight interaction between the cell membrane and the polymer. With this in mind, we hypothesized that the electron-dense vesicles (Figure 2e–g) and the Toluidine Blue-positive structures (Figure 2d) observed in the first days of culture of the aggregates by TEM and by optical microscopy analysis, respectively, are vesicular structures containing the polymer internalized through the cell membrane.

To support this, let us recall the strong affinity of CTL for osmium tetroxide[38] and the weak affinity of Toluidine Blue for CTL (data not shown).

To test this hypothesis, chondrocytes were cultured in the presence and absence of CTL, both in adhesion and in the form of aggregates, and analyzed by means of optical and electron microscopy (Figures 4a and S2, Supporting Information).

As expected, in chondrocytes in adhesion (Figures 4b and S2, Supporting Information) and in spheroids grown in the absence of CTL (Figures 4c and S2, Supporting Information), no vesicles or granules were visible on TEM and in optical microscopy images. In contrast, on TEM and in optical microscopy of adherent chondrocytes cultured in the presence of CTL solution, electrodense vesicles and granules (yellow arrows in Figure 4d and red arrows in Figure S2, Supporting Information) similar to those seen in chondro-aggregates formed with CTL are visible. The presence of these cytoplasmic structures only in cells in contact with the polymer almost certainly indicates that they are the result of the process of internalization of the polysaccharide by the chondrocytes.

As further evidence of CTL uptake within the cells, flow cytometry analysis was performed on isolated chondrocytes incubated with CTL labeled with FITC. To discriminate between cell association and actual internalization, extracellular fluorescence was quenched by the addition of trypan blue, the nonquenched fraction thus representing cells with internalized polymer. Cells treated with CTL were analyzed before and after the addition of the quenching agent. By superimposing the histogram of the fluorescence of the cells without trypan blue on the histogram of the fluorescence of the cells in the presence of the quencher made it possible to estimate that almost 80% of the fluorescent polymer is intracellular (Figure S3a, Supporting Information). Moreover, confocal microscopy analyses of free chondrocytes incubated with FITC–CTL confirmed these results. In particular, the observation of the cells in different Z-stacks allowed the identification of the fluorescence of the polymer also inside the cells (Figure S3b, Supporting Information).

3.4. Chondro-Aggregates Adhesion and Chondrocytes Migration. The ability of chondrocytes to migrate out of the aggregate structure and adhere and spread on culture wells was investigated with a cell migration assay. For this purpose, the formation of chondro-aggregates on a CTL-

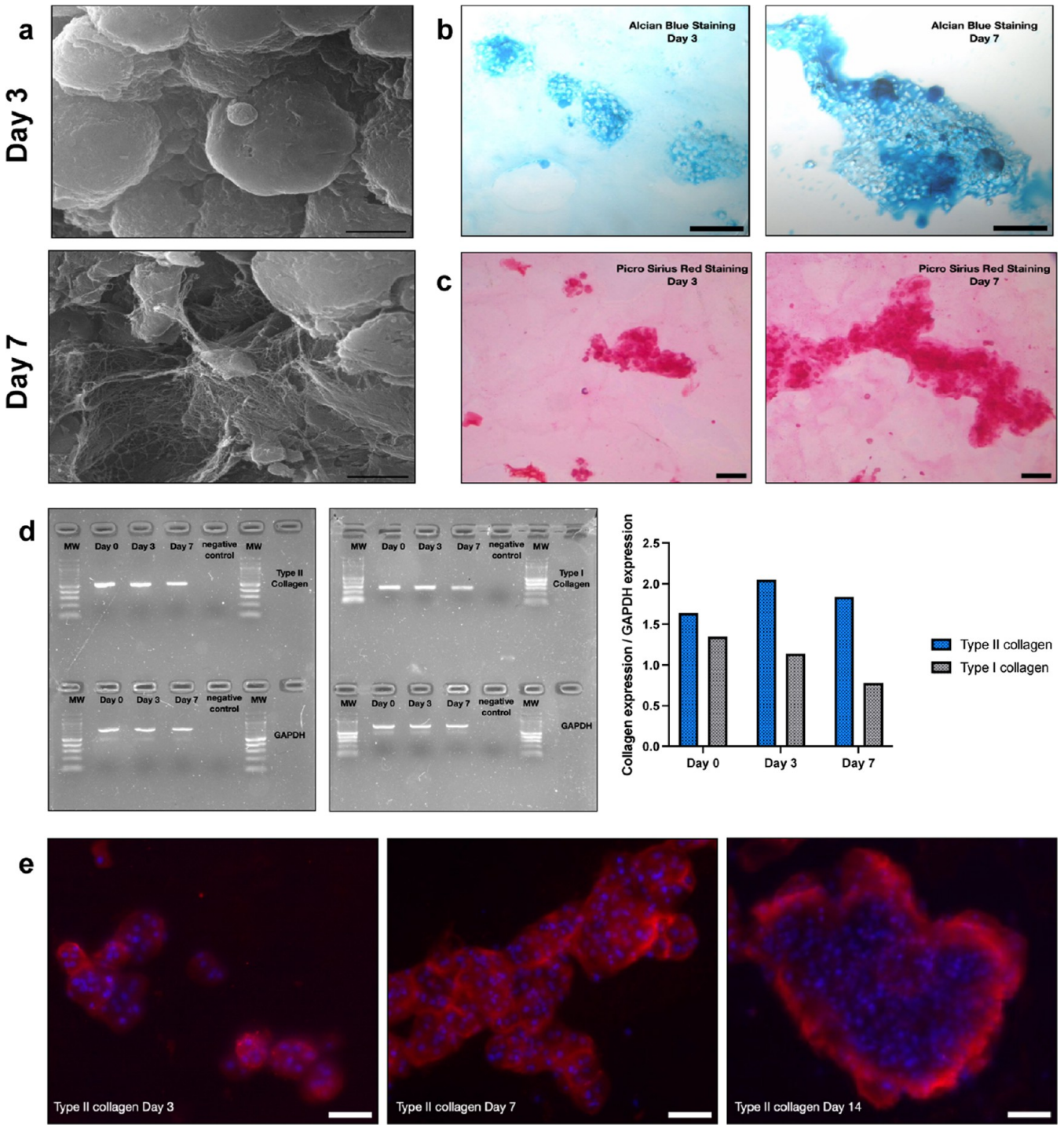

Figure 6. Extracellular matrix deposition in chondro-aggregates. (a) SEM images of chondrocytes after 3 and 7 days of culture (scale bar 5 μm). (b) Alcian Blue and (c) Picro Sirius Red staining of aggregates at days 3 and 7 (scale bar 50 μm). (d) COL2A1 and COL1A2 gene expressions by RT-PCR; the relative intensity of DNA bands was analyzed by ImageJ software and normalized over GAPDH expression. (e) Immunohistochemical images of type II collagen deposition at different time points. Nuclei were stained with Hoechst (blue) (scale bar 50 μm).

coated well was performed according to the procedure described in Section 2.3, and the aggregates at different time points were transferred to plate wells without any coating. This test allowed us to simulate the ability of cells composing the chondro-aggregates to colonize the cartilage defect and potentially allow tissue regeneration in situ.[39] The relocation of aggregates on the noncoated wells was performed 1, 3, and 7 days after their formation, and the ability of the cells to migrate out of the structure and adhere was evaluated through an optical microscope. The optical images show that the chondro-aggregates adhere to the bottom of the wells and that the cells composing the aggregates are able to migrate out of the aggregate structure and spread on the surface of the well, albeit to an extent that depends on the timing of transfer to the uncoated well after formation. When the chondro-aggregates are transferred to the uncoated well 1 and 3 days after formation, they can adhere to the surface of the well regardless of the size of the aggregates (Figure 5a,b). In the case of the 3

day chondro-aggregates, the chondrocytes were able to migrate out of the aggregates and also colonize the entire surface, reaching cell confluency after 10 days. In contrast, for the chondro-aggregates that were transferred after 7 days of culture, aggregate adhesion was impaired for the larger aggregates that remained in suspension, while only the smaller ones are able to adhere (Figure 5c). In the latter case, the number of chondrocytes moving out of the aggregates was lower than in the 3 day aggregates and reduced surface colonization occurred over time. Overall, these results show that CTL chondro-aggregates cultured for up to 7 days are able to adhere to a permissive surface and migrate out of the aggregate structure; extensive surface colonization by cells that migrated out of the aggregate structure occurred only in the 3 day chondro-aggregates.

3.5. Matrix Production and Bioactive Properties of CTL. To assess the deposition of ECM by the chondrocytes in the chondro-aggregates, a qualitative analysis was performed. Since the chondro-aggregates were able to adhere to a permissive surface for up to 7 days, this period was considered for the assessment of ECM production. The ultrastructural TEM analysis showed an increase in collagen fibrils at days 7 and 14 (Figure 2g). This increase in matrix deposition is also confirmed by SEM analyses. At higher magnification, the chondrocytes appear embedded in a filamentous matrix that increases over time (Figure 6a). Histological staining, immunohistochemistry, and gene analysis were used to obtain information about the components of the ECM. For this purpose, the aggregates were stained with Alcian Blue and Picro Sirius Red to investigate the production of GAGs (Figure 6b) and collagen (Figure 6c), respectively. These two stains show an increase in matrix deposition between the two time points examined. Detailed information on the type of collagen composing the matrix (i.e., type I and type II collagen) was obtained by gene expression analyses and immunohistochemical studies (Figure 6d,e). A semiquantitative analysis of the gene expression of collagen II was performed by polymerase chain reaction (PCR) and showed that the production of this marker increases with time. This result was also confirmed by immunohistochemical analyses, which showed that matrix production increased during the 14 day culture, especially on the outside of the structure. On the other hand, as far as the production of type I collagen, its expression decreases at the genetic level and its presence detected by the use of the antibody is very low (Figure S4, Supporting Information).

4. DISCUSSION

In recent years, chondro-spheroids, i.e., self-aggregated spheroids derived from chondrocytes cultured without biomaterials or ECM components to support cell-to-cell attachment, have been identified in the scientific literature as efficient systems for clinical regeneration of cartilage in the technique known as ACI. Scaffold-free products such as Chondrosphere have shown promising results in clinical practice.[4,40,41]

The bioactive properties of CTL and its ability to induce cell aggregation[17,42] have been widely reported in the literature, both *in vitro* and *in vivo*.[20,23,24,29,30,43−46]

These properties can be traced back to the high accessibility of the terminal galactose in the side chain for specific galactose-binding proteins such as Gal-1 and underline its biological potential in the field of tissue regeneration.[25]

Given the data and experimental evidence described above, it seemed of interest in this work to characterize in detail the structure and morphology of chondro-aggregates and their process of formation in the presence of CTL.[17] In particular, this study focused on the influence of the polymer on the formation of the aggregates and on the close structural and functional interaction that takes place between the polymeric and cellular components, with the aim to develop a scaffold-free cell system that could promote cartilage regeneration.

In scaffold-free spheroids, cell aggregation is promoted by cell-to-cell adhesion, and in this forced self-assembly process, cells secrete their own ECM components. As the 3D culture methods described in the literature are various,[35,47] the resulting spheroids may vary slightly in size, morphology, and complexity. However, most chondro-spheroids reach a size of 900−1000 μm in the first days of aggregation. The structure remains uniformly spherical and appears to be uniformly compact and it is characterized by cells that are in close contact with each other.[39] Spheroids are homogeneous, well-rounded, and solid cell aggregates.[48,49] Over time, shrinkage of the spheroids and the formation of a necrotic core are often observed as the ability of the cells to proliferate is compromised.[48] This behavior is also described in the literature for spheroids formed by other primary cells and cell lines as well as by mesenchymal stem cells (MSCs).[50,51] The dynamic process of chondro-aggregates formation in the presence of CTL appears to be substantially different from the one described in the literature, where cell aggregation occurs by preventing cell adhesion on a substrate. Rather, in the case of CTL, the polymer itself is the scaffold fostering cell aggregation. From the first days of culture, the cells do not appear densely packed and the spheroids, which are initially numerous, well distributed, and very small (200−300 μm), quickly lose their spherical shape and increase in size, mainly due to a slow coalescence process of the preexisting nodules (Figures 1 and 2a−c). While cell−cell interactions mediated initially by integrins and later by cadherins predominate in the literature,[37] chondrocytes in the presence of CTL do not interact directly with each other but are interspersed with the presence of an amorphous matrix formed by CTL without direct cell−cell contacts (Figures 2a−c and 3a,b).

The presence and the close interaction between the cells and the polymer both outside and inside the structure (Figure 3a,b) seem to indicate that CTL plays an active role in the formation of these chondro-aggregates by acting as a structuring temporary extracellular matrix. The process of chondro-aggregates formation in the presence of CTL can probably be explained by an initial phase in which the polymer fibers act as long-chain linkers for the attachment of dispersed single cells to form loose aggregates, probably through the binding of integrins with lactose pending groups. Over time, concomitant with the process of fusion of the aggregates and the concomitant increase in their size (Figure 1), a progressive uprise in the content of endogenous type II collagen synthesis in the extracellular matrix is observed (Figure 6). Although proliferative capacity is limited (Figure 1b), cell viability appears to be good during the first 14 days of culture. The formation of a necrotic core within the larger aggregates is probably related to the poor diffusion capacity of respiratory gases and nutrients (Figure 1c). In Figure 2c, it is interesting to observe the rearrangement of the cell in a crown structure in which much of the cartilage matrix appears concentrated (Figure 6). In contrast, CTL is concentrated in the partially

necrotic core as an amorphous polymeric matrix (Figures 2c and 3b). While the CTL initially appears to act as a biological glue, it is gradually replaced by a newly secreted extracellular matrix as the chondro-aggregates mature (Figures 3 and 6).

In the clinical application of chondro-spheroids, the migration of cells from the spheroid and their adhesive and colonizing properties toward cartilage and subchondral tissue are considered essential for therapeutic purposes.[39,52]

Herein, we find that the presence of the polymer did not affect the adhesiveness of the chondro-aggregates and the migratory ability of the chondrocytes when transferred to standard tissue culture plastic, although the ability to colonize the surfaces is closely related to the age and size of the structures (Figure 5). The process of complete adhesion, migration, spreading, and cell proliferation is observed in chondro-aggregates transferred 3 days after their formation. Over time, they lose this ability. As described in Section 3.1, over time the aggregates tend to aggregate with each other. Aggregation involves the formation of numerous cell−cell, cell−matrix, and cell−polymer interactions. The chondrocytes then become bound into a compact structure, which impairs migration when in contact with plastic. One of the most interesting aspects highlighted by this study is the ability of chondrocytes, both free and in the form of aggregates, to internalize CTL into vesicular structures (Figure 4). This close interaction between CTL and chondrocytes does not affect the viability of the aggregates (Figure 1c,d), reflecting the biocompatibility of this polymer. The internalization process only occurs during the first few days of culture, and the polymer is then metabolized by the chondrocytes themselves. As can be seen in Figure 2, the electrodense vesicles containing the polymer actually decreased after 2 weeks. The process of intracellular CTL degradation is not yet known, but in analogy to what has been reported for the polymer chitosan,[53−55] acid hydrolysis, oxidation, and the action of nonspecific enzymes such as lysozyme[21] and/or other glycosidases are probably involved. In the future, it would be very interesting to study in detail the mechanism of internalization of the polymer by chondrocytes and to evaluate the possible role of glycosidases. Indeed, some studies have discussed the role of hexosaminidases as the predominant glycosidases in the degradation of GAGs in cartilage degeneration processes.[56,57] The search for inhibitors of this enzyme could be a good strategy for the prevention and treatment of cartilage degeneration.[58] Future studies will aim to investigate ex vivo and in vivo the regenerative capacity of chondrocytes entrapped in the CTL matrix. Particular attention will be paid to evaluating the synergistic effect that a hybrid system delivering both cells and a bioactive molecule might have in promoting the healing process.

5. CONCLUSIONS

The promotion of cell aggregation by a lactose-modified chitosan (CTL) has been reported in the literature. Due to the bioactive properties of this polymer and its chondroprotective potential, in the present work, we focused on the role of the polymer in spheroid formation and on the possible application of this type of chondro-aggregates in cartilage regeneration. The assembly of the structures occurs spontaneously and seems to be related to and controlled by CTL and its close molecular interaction with the cells. CTL has a high cellular affinity and biocompatibility, so it is internalized and metabolized by chondrocytes. Although initially surrounded by a CTL matrix, the cells synthesize their own collagen-type extracellular matrix, which gradually replaces the synthetic matrix. In the structures, cells retain the ability to migrate and colonize the surrounding surface during short culture periods. The subsequent disaggregation of the spheroidal structure would favor the release of the bioactive polymer CTL *in situ*. CTL-based chondro-aggregates would represent a novelty in the field of scaffold-free regenerative approaches for cartilage known as ACI. Indeed, they combine all of the advantages of traditional ACI techniques with the ability to impart a proregenerative bioactive component to the damaged site through a simple cellular system. A forthcoming study is necessary to compare this type of chondro-aggregates with chondro-spheroids already used in clinical practice to investigate the advantages of these cellular systems over conventional methods based on chondro-spheroids.

■ ASSOCIATED CONTENT

Supporting Information

The Supporting Information is available free of charge at https://pubs.acs.org/doi/10.1021/acsapm.2c01613.

List of primers for polymerase chain reaction (PCR) (Table S1); a figure of LDH assay on chondro-aggregates at different time points (Figure S1); a figure of CTL internalization (Figure S2); a figure of the analysis of CTL internalized by chondrocytes (Figure S3); and a figure of immunohistochemical images of collagen type I at different time points on sectioned chondro-aggregates (Figure S4) (PDF)

■ AUTHOR INFORMATION

Corresponding Author

Francesca Scognamiglio − *Department of Medical, Surgical and Health Sciences, University of Trieste, 34129 Trieste, Italy;* orcid.org/0000-0003-4968-2105; Phone: 0039-0405588731; Email: fscognamiglio@units.it

Authors

Chiara Pizzolitto − *Department of Medical, Surgical and Health Sciences, University of Trieste, 34129 Trieste, Italy;* orcid.org/0000-0001-9178-600X

Giovanna Baldini − *Department of Medical, Surgical and Health Sciences, University of Trieste, 34129 Trieste, Italy*

Roberta Bortul − *Department of Medical, Surgical and Health Sciences, University of Trieste, 34129 Trieste, Italy*

Gianluca Turco − *Department of Medical, Surgical and Health Sciences, University of Trieste, 34129 Trieste, Italy;* orcid.org/0000-0001-5699-2131

Ivan Donati − *Department of Life Sciences, University of Trieste, 34127 Trieste, Italy;* orcid.org/0000-0003-3752-8346

Vanessa Nicolin − *Department of Medical, Surgical and Health Sciences, University of Trieste, 34129 Trieste, Italy*

Eleonora Marsich − *Department of Medical, Surgical and Health Sciences, University of Trieste, 34129 Trieste, Italy;* orcid.org/0000-0002-0700-4464

Funding

This research did not receive any specific grant from funding agencies in the public, commercial, or not-for-profit sectors.

Notes

The authors declare no competing financial interest.

The authors declare the following financial interests/personal relationships, which may be considered potential competing interests: the authors Eleonora Marsich, Gianluca Turco, and Ivan Donati declare to be shareholders of the company BiopoLife S.r.l. The authors confirm that there has been no financial support for this work that could have influenced its outcome.

■ ACKNOWLEDGMENTS

The authors thank the Department of Medical, Surgical and Health Sciences, University of Trieste, for the financial support to F.S. (Fellowship: "Materiali meccanotrasduttivi: studio degli effetti sul differenziamento di cellule mesenchimali") and Macelleria F.lli De Colle, Coderno di Sedegliano (UD, Italy), for kindly providing intact joints of adult pigs.

■ REFERENCES

(1) Chen, A.; Gupte, C.; Akhtar, K.; Smith, P.; Cobb, J. The Global Economic Cost of Osteoarthritis: How the UK Compares. *Arthritis* **2012**, *2012*, 1−6.

(2) Hiligsmann, M.; Cooper, C.; Guillemin, F.; Hochberg, M. C.; Tugwell, P.; Arden, N.; Berenbaum, F.; Boers, M.; Boonen, A.; Branco, J. C.; Maria-Luisa, B.; Bruyère, O.; Gasparik, A.; Kanis, J. A.; Kvien, T. K.; Martel-Pelletier, J.; Pelletier, J. P.; Pinedo-Villanueva, R.; Pinto, D.; Reiter-Niesert, S.; Rizzoli, R.; Rovati, L. C.; Severens, J. L.; Silverman, S.; Reginster, J. Y. A Reference Case for Economic Evaluations in Osteoarthritis: An Expert Consensus Article from the European Society for Clinical and Economic Aspects of Osteoporosis and Osteoarthritis (ESCEO). *Semin. Arthritis Rheum.* **2014**, *44*, 271−282.

(3) Makris, E. A.; Gomoll, A. H.; Malizos, K. N.; Hu, J. C.; Athanasiou, K. A. Repair and Tissue Engineering Techniques for Articular Cartilage. *Nat. Rev. Rheumatol.* **2015**, *11*, 21−34.

(4) Jiang, S.; Guo, W.; Tian, G.; Luo, X.; Peng, L.; Liu, S.; Sui, X.; Guo, Q.; Li, X. Clinical Application Status of Articular Cartilage Regeneration Techniques: Tissue-Engineered Cartilage Brings New Hope. *Stem Cells Int.* **2020**, *2020*, No. 5690252.

(5) Ossendorf, C.; Kaps, C.; Kreuz, P. C.; Burmester, G. R.; Sittinger, M.; Erggelet, C. Treatment of Posttraumatic and Focal Osteoarthritic Cartilage Defects of the Knee with Autologous Polymer-Based Three-Dimensional Chondrocyte Grafts: 2-Year Clinical Results. *Arthritis Res. Ther.* **2007**, *9*, 1−11.

(6) Brix, M. O.; Stelzeneder, D.; Chiari, C.; Koller, U.; Nehrer, S.; Dorotka, R.; Windhager, R.; Domayer, S. E. Treatment of Full-Thickness Chondral Defects with Hyalograft C in the Knee: Long-Term Results. *Am. J. Sports Med.* **2014**, *42*, 1426−1432.

(7) Crawford, D. C.; DeBerardino, T. M.; Williams, R. J. NeoCart, an Autologous Cartilage Tissue Implant, Compared with Microfracture for Treatment of Distal Femoral Cartilage Lesions. *J. Bone Jt. Surg.* **2012**, *94*, 979−989.

(8) Hulme, C. H.; Perry, J.; McCarthy, H. S.; Wright, K. T.; Snow, M.; Mennan, C.; Roberts, S. Cell Therapy for Cartilage Repair. *Emerg. Top. Life Sci.* **2021**, *5*, 575−589.

(9) Huang, B. J.; Hu, J. C.; Athanasiou, K. A. Cell-Based Tissue Engineering Strategies Used in the Clinical Repair of Articular Cartilage. *Biomaterials* **2016**, *98*, 1−22.

(10) Pestka, J. M.; Schmal, H.; Salzmann, G.; Hecky, J.; Südkamp, N. P.; Niemeyer, P. In Vitro Cell Quality of Articular Chondrocytes Assigned for Autologous Implantation in Dependence of Specific Patient Characteristics. *Arch. Orthop. Trauma Surg.* **2011**, *131*, 779−789.

(11) Pietschmann, M. F.; Niethammer, T. R.; Horng, A.; Gülecyüz, M. F.; Feist-Pagenstert, I.; Jansson, V.; Müller, P. E. The Incidence and Clinical Relevance of Graft Hypertrophy after Matrix-Based Autologous Chondrocyte Implantation. *Am. J. Sports Med.* **2012**, *40*, 68−74.

(12) Choi, J. R.; Yong, K. W.; Choi, J. Y. Effects of Mechanical Loading on Human Mesenchymal Stem Cells for Cartilage Tissue Engineering. *J. Cell Physiol.* **2018**, *233*, 1913−1928.

(13) Vonk, L. A.; Roël, G.; Hernigou, J.; Kaps, C.; Hernigou, P. Role of Matrix-associated Autologous Chondrocyte Implantation with Spheroids in the Treatment of Large Chondral Defects in the Knee: A Systematic Review. *Int. J. Mol. Sci.* **2021**, *22*, No. 7149.

(14) Cheng, N. C.; Wang, S.; Young, T. H. The Influence of Spheroid Formation of Human Adipose-Derived Stem Cells on Chitosan Films on Stemness and Differentiation Capabilities. *Biomaterials* **2012**, *33*, 1748−1758.

(15) Huang, G. S.; Dai, L. G.; Yen, B. L.; Hsu, S. hui. Spheroid Formation of Mesenchymal Stem Cells on Chitosan and Chitosan-Hyaluronan Membranes. *Biomaterials* **2011**, *32*, 6929−6945.

(16) Kronemberger, G. S.; Matsui, R. A. M.; de Castro e Miranda, G. A. S.; Granjeiro, J. M.; Baptista, L. S. Cartilage and Bone Tissue Engineering Using Adipose Stromal/Stem Cells Spheroids as Building Blocks. *World J. Stem Cells* **2020**, *12*, 110−122.

(17) Donati, I.; Stredanska, S.; Silvestrini, G.; Vetere, A.; Marcon, P.; Marsich, E.; Mozetic, P.; Gamini, A.; Paoletti, S.; Vittur, F. The Aggregation of Pig Articular Chondrocyte and Synthesis of Extracellular Matrix by a Lactose-Modified Chitosan. *Biomaterials* **2005**, *26*, 987−998.

(18) Sacco, P.; Cok, M.; Scognamiglio, F.; Pizzolitto, C.; Vecchies, F.; Marfoglia, A.; Marsich, E.; Donati, I. Glycosylated-Chitosan Derivatives: A Systematic Review. *Molecules* **2020**, *25*, 1534.

(19) D'Amelio, N.; Esteban, C.; Coslovi, A.; Feruglio, L.; Uggeri, F.; Villegas, M.; Benegas, J.; Paoletti, S.; Donati, I. Insight into the Molecular Properties of Chitlac, a Chitosan Derivative for Tissue Engineering. *J. Phys. Chem. B* **2013**, *117*, 13578−13587.

(20) Marsich, E.; Borgogna, M.; Donati, I.; Mozetic, P.; Strand, B. L.; Salvador, S. G.; Vittur, F.; Paoletti, S. Alginate/Lactose-Modified Chitosan Hydrogels: A Bioactive Biomaterial for Chondrocyte Encapsulation. *J. Biomed. Mater. Res., Part A* **2008**, *84*, 364−376.

(21) Scognamiglio, F.; Travan, A.; Donati, I.; Borgogna, M.; Marsich, E. A Hydrogel System Based on a Lactose-Modified Chitosan for Viscosupplementation in Osteoarthritis. *Carbohydr. Polym.* **2020**, *248*, No. 116787.

(22) Tarricone, E.; Mattiuzzo, E.; Belluzzi, E.; Elia, R.; Benetti, A.; Venerando, R.; Vindigni, V.; Ruggieri, P.; Brun, P. Anti-Inflammatory Performance of Lactose-Modified Osteoarthritis Model. *Cells* **2020**, *9*, 1328.

(23) Salamanna, F.; Giavaresi, G.; Parrilli, A.; Martini, L.; Nicoli Aldini, N.; Abatangelo, G.; Frizziero, A.; Fini, M. Effects of Intra-Articular Hyaluronic Acid Associated to Chitlac (Arty-Duo) in a Rat Knee Osteoarthritis Model. *J. Orthop. Res.* **2019**, *37*, 867−876.

(24) Tschon, M.; Salamanna, F.; Martini, L.; Giavaresi, G.; Lorenzini, L.; Calzà, L.; Fini, M. Boosting the Intra-Articular Efficacy of Low Dose Corticosteroid through a Biopolymeric Matrix: An In Vivo Model of Osteoarthritis. *Cells* **2020**, *9*, 1−16.

(25) Marcon, P.; Marsich, E.; Vetere, A.; Mozetic, P.; Campa, C.; Donati, I.; Vittur, F.; Gamini, A.; Paoletti, S. The Role of Galectin-1 in the Interaction between Chondrocytes and a Lactose-Modified Chitosan. *Biomaterials* **2005**, *26*, No. 4975.

(26) Liu, Q.; Sacco, P.; Marsich, E.; Furlani, F.; Arib, C.; Djaker, N.; Lamy De La Chapelle, M.; Donati, I.; Spadavecchia, J. Lactose-Modified Chitosan Gold(III)-PEGylated Complex-Bioconjugates: From Synthesis to Interaction with Targeted Galectin-1 Protein. *Bioconjugate Chem.* **2018**, *29*, 3352−3361.

(27) Osório, J. Osteoarthritis: Galectin-1 Damages Cartilage via Inflammation. *Nat. Rev. Rheumatol.* **2016**, *12*, 132−133.

(28) Toegel, S.; Weinmann, D.; André, S.; Walzer, S. M.; Bilban, M.; Schmidt, S.; Chiari, C.; Windhager, R.; Krall, C.; Bennani-Baiti, I. M.; Gabius, H.-J. Galectin-1 Couples Glycobiology to Inflammation in Osteoarthritis through the Activation of an NF-KB−Regulated Gene Network. *J. Immunol.* **2016**, *196*, 1910−1921.

(29) Donato, A.; Belluzzi, E.; Mattiuzzo, E.; Venerando, R.; Cadamuro, M.; Ruggieri, P.; Vindigni, V.; Brun, P. Anti-Inflammatory and Pro-Regenerative Effects of Hyaluronan-Chitlac Mixture in Human Dermal Fibroblasts: A Skin Ageing Perspective. *Polymers* **2022**, *14*, No. 1817.
(30) Tarricone, E.; Mattiuzzo, E.; Belluzzi, E.; Elia, R.; Benetti, A.; Venerando, R.; Vindigni, V.; Ruggieri, P.; Brun, P. Anti-Inflammatory Performance of Lactose-Modified Chitosan and Hyaluronic Acid Mixtures in an In Vitro Macrophage-Mediated Inflammation Osteoarthritis Model. *Cells* **2020**, *9*, No. 1328.
(31) Scognamiglio, F.; Travan, A.; Borgogna, M.; Donati, I.; Marsich, E. Development of Biodegradable Membranes for the Delivery of a Bioactive Chitosan-Derivative on Cartilage Defects: A Preliminary Investigation. *J. Biomed. Mater. Res., Part A* **2020**, *108*, 1534−1545.
(32) Grandolfo, M.; D'Andrea, P.; Paoletti, S.; Martina, M.; Silvestrini, G.; Bonucci, E.; Vittur, F. Culture and Differentiation of Chondrocytes Entrapped in Alginate Gels. *Calcif. Tissue Int.* **1993**, *52*, 42−48.
(33) Chaudhuri, O.; Gu, L.; Klumpers, D.; Darnell, M.; Sidi, A.; Weaver, J. C.; Huebsch, N.; Lee, H.; Lippens, E.; Duda, G. N.; Mooney, D. J. Hydrogels with Tunable Stress Relaxation Regulate Stem Cell Fate and Activity. *Nat. Mater.* **2016**, *15*, 326−334.
(34) Sacco, P.; Brun, F.; Donati, I.; Porrelli, D.; Paoletti, S.; Turco, G. On the Correlation between the Microscopic Structure and Properties of Phosphate-Cross-Linked Chitosan Gels. *ACS Appl. Mater. Interfaces* **2018**, *10*, 10761−10770.
(35) Ryu, N. E.; Lee, S. H.; Park, H. Spheroid Culture System Methods and Applications for Mesenchymal Stem Cells. *Cells* **2019**, *8*, 1−13.
(36) Białkowska, K.; Komorowski, P.; Bryszewska, M.; Miłowska, K. Spheroids as a Type of Three-Dimensional Cell Cultures—Examples of Methods of Preparation and the Most Important Application. *Int. J. Mol. Sci.* **2020**, *21*, 1−17.
(37) Lin, R. Z.; Chou, L. F.; Chien, C. C. M.; Chang, H. Y. Dynamic Analysis of Hepatoma Spheroid Formation: Roles of E-Cadherin and B1-Integrin. *Cell Tissue Res.* **2006**, *324*, 411−422.
(38) Brun, F.; Accardo, A.; Marchini, M.; Ortolani, F.; Turco, G.; Paoletti, S. Texture Analysis of TEM Micrographs of Alginate Gels for Cell Microencapsulation. *Microsc. Res. Tech.* **2011**, *74*, 58−66.
(39) Anderer, U.; Libera, J. In Vitro Engineering of Human Autogenous Cartilage. *J. Bone Miner. Res.* **2002**, *17*, 1420−1429.
(40) Armoiry, X.; Cummins, E.; Connock, M.; Metcalfe, A.; Royle, P.; Johnston, R.; Rodrigues, J.; Waugh, N.; Mistry, H. Autologous Chondrocyte Implantation with Chondrosphere for Treating Articular Cartilage Defects in the Knee: An Evidence Review Group Perspective of a NICE Single Technology Appraisal. *Pharmacoeconomics* **2019**, *37*, 879−886.
(41) Grevenstein, D.; Mamilos, A.; Schmitt, V. H.; Niedermair, T.; Wagner, W.; Kirkpatrick, C. J.; Brochhausen, C. Excellent Histological Results in Terms of Articular Cartilage Regeneration after Spheroid-Based Autologous Chondrocyte Implantation (ACI). *Knee Surg., Sports Traumatol. Arthrosc.* **2021**, *29*, 417−421.
(42) Pizzolitto, C.; Esposito, F.; Sacco, P.; Marsich, E.; Gargiulo, V.; Bedini, E.; Donati, I. Sulfated Lactose-Modified Chitosan. A Novel Synthetic Glycosaminoglycan-like Polysaccharide Inducing Chondrocyte Aggregation. *Carbohydr. Polym.* **2022**, *288*, No. 119379.
(43) Travan, A.; Donati, I.; Marsich, E.; Bellomo, F.; Achanta, S.; Toppazzini, M.; Semeraro, S.; Scarpa, T.; Spreafico, V.; Paoletti, S. Surface Modification and Polysaccharide Deposition on BisGMA/TEGDMA Thermoset. *Biomacromolecules* **2010**, *11*, 583−592.
(44) Medelin, M.; Porrelli, D.; Aurand, E. R.; Scaini, D.; Travan, A.; Borgogna, M. A.; Cok, M.; Donati, I.; Marsich, E.; Scopa, C.; Scardigli, R.; Paoletti, S.; Ballerini, L. Exploiting Natural Polysaccharides to Enhance in Vitro Bio-Constructs of Primary Neurons and Progenitor Cells. *Acta Biomater.* **2018**, *73*, 285−301.
(45) Rapino, M.; Di Valerio, V.; Zara, S.; Gallorini, M.; Marconi, G. D.; Sancilio, S.; Marsich, E.; Ghinassi, B.; Di Giacomo, V.; Cataldi, A. Chitlac-Coated Thermosets Enhance Osteogenesis and Angiogenesis in a Co-Culture of Dental Pulp Stem Cells and Endothelial Cells. *Nanomaterials* **2019**, *9*, No. 928.
(46) Tarricone, E.; Elia, R.; Mattiuzzo, E.; Faggian, A.; Pozzuoli, A.; Ruggieri, P.; Brun, P. The Viability and Anti-Inflammatory Effects of Hyaluronic Acid-Chitlac-Tracimolone Acetonide- β-Cyclodextrin Complex on Human Chondrocytes. *Cartilage* **2021**, *13*, 920S−924S.
(47) Velasco, V.; Shariati, S. A.; Esfandyarpour, R. Microtechnology-Based Methods for Organoid Models. *Microsyst. Nanoeng.* **2020**, *6*, No. 672.
(48) Martinez, I.; Elvenes, J.; Olsen, R.; Bertheussen, K.; Johansen, O. Redifferentiation of in Vitro Expanded Adult Articular Chondrocytes by Combining the Hanging-Drop Cultivation Method with Hypoxic Environment. *Cell Transplant.* **2008**, *17*, 987−996.
(49) Gryadunova, A.; Kasamkattil, J.; Gay, M. H. P.; Dasen, B.; Pelttari, K.; Mironov, V.; Martin, I.; Schären, S.; Barbero, A.; Krupkova, O.; Mehrkens, A. Nose to Spine: Spheroids Generated by Human Nasal Chondrocytes for Scaffold-Free Nucleus Pulposus Augmentation. *Acta Biomater.* **2021**, *134*, 240−251.
(50) Zubillaga, V.; Alonso-varona, A.; Fernandes, S. C. M.; Salaberria, A. M.; Palomares, T. Adipose-Derived Mesenchymal Stem Cell Chondrospheroids Cultured in Hypoxia and a 3D Porous Chitosan/Chitin Nanocrystal Scaffold as a Platform for Cartilage Tissue Engineering. *Int. J. Mol. Sci.* **2020**, *21*, 1−17.
(51) Cesarz, Z.; Tamama, K. Spheroid Culture of Mesenchymal Stem Cells. *Stem Cells Int.* **2016**, *2016*, No. 9176357.
(52) Omelyanenko, N. P.; Karalkin, P. A.; Bulanova, E. A.; Koudan, E. V.; Parfenov, V. A.; Rodionov, S. A.; Knyazeva, A. D.; Kasyanov, V. A.; Babichenko, I. I.; Chkadua, T. Z.; Khesuani, Y. D.; Gryadunova, A. A.; Mironov, V. A. Extracellular Matrix Determines Biomechanical Properties of Chondrospheres during Their Maturation In Vitro. *Cartilage* **2020**, *11*, 521−531.
(53) Islam, N.; Dmour, I.; Taha, M. O. Degradability of Chitosan Micro/Nanoparticles for Pulmonary Drug Delivery. *Heliyon* **2019**, *5*, No. e01684.
(54) Kulish, E. I.; Volodina, V. P.; Fatkullina, R. R.; Kolesov, S. V.; Zaikov, G. E. Enzymatic Degradation of Chitosan Films under the Action of Nonspecific Enzymes. *Polym. Sci., Ser. B* **2008**, *50*, 175−176.
(55) Du, H.; Yang, X.; Zhai, G. Design of Chitosan-Based Nanoformulations for Efficient Intracellular Release of Active Compounds. *Nanomedicine* **2014**, *9*, 723−740.
(56) Shikhman, A. R.; Brinson, D. C.; Lotz, M. Profile of Glycosaminoglycan-Degrading Glycosidases and Glycoside Sulfatases Secreted by Human Articular Chondrocytes in Homeostasis and Inflammation. *Arthritis Rheumatol.* **2000**, *43*, 1307−1314.
(57) Pásztói, M.; Nagy, G.; Géher, P.; Lakatos, T.; Tóth, K.; Wellinger, K.; Pócza, P.; György, B.; Holub, M. C.; Kittel, Á.; Pálóczy, K.; Mazán, M.; Nyirkos, P.; Falus, A.; Buzas, E. I. Gene Expression and Activity of Cartilage Degrading Glycosidases in Human Rheumatoid Arthritis and Osteoarthritis Synovial Fibroblasts. *Arthritis Res. Ther.* **2009**, *11*, 1−13.
(58) Liu, J.; Shikhman, A. R.; Lotz, M. K.; Wong, C. H. Hexosaminidase Inhibitors as New Drug Candidates for the Therapy of Osteoarthritis. *Chem. Biol.* **2001**, *8*, 701−711.